Nonperturbative shell-model interactions from the in-medium similarity renormalization group

S. K. Bogner,[1, *] H. Hergert,[2, †] J. D. Holt,[3, 4, 1, ‡] A. Schwenk,[3, 4, §]
S. Binder,[4] A. Calci,[4] J. Langhammer,[4] and R. Roth[4]

[1] *National Superconducting Cyclotron Laboratory and Department of Physics and Astronomy,*
Michigan State University, East Lansing, MI 48844, USA
[2] *Department of Physics, The Ohio State University, Columbus, OH 43210, USA*
[3] *ExtreMe Matter Institute EMMI, GSI Helmholtzzentrum für Schwerionenforschung GmbH, 64291 Darmstadt, Germany*
[4] *Institut für Kernphysik, Technische Universität Darmstadt, 64289 Darmstadt, Germany*

We present the first *ab initio* construction of valence-space Hamiltonians for medium-mass nuclei based on chiral two- and three-nucleon interactions using the in-medium similarity renormalization group. When applied to the oxygen isotopes, we find good agreement with experimental ground-state energies, including the flat trend beyond the drip line at ^{24}O. Similarly, even-parity spectra in ^{21,22,23,24}O are in excellent agreement with experiment, and we present predictions for excited states in ^{25,26}O. The results exhibit a weak dependence on the harmonic-oscillator basis parameter and give a good description of spectroscopy within the standard sd valence space.

Introduction. With the next generation of rare-isotope beam facilities, the quest to discover and understand the properties of exotic nuclei from first principles represents a fundamental challenge for nuclear theory. This challenge is complicated in part because the proper inclusion of three-nucleon (3N) forces plays a decisive role in determining the structure of medium-mass nuclei [1, 2]. While *ab initio* many-body methods based on nuclear forces from chiral effective field theory (EFT) [3–5] have now reached the medium-mass region and beyond [6–19], restrictions in the nuclei and observables accessible to these methods have limited their scope primarily to ground-state properties in semi-magic isotopic chains.

For open-shell systems with many valence nucleons, rather than attempting to solve the full A-body problem, it is profitable to follow the shell-model paradigm by constructing and diagonalizing an effective Hamiltonian in which the active degrees of freedom are the A_v valence nucleons confined to a few orbitals near the Fermi level. Both phenomenological and microscopically based implementations of the shell model have been used with great success to understand and predict nuclear structure, including the evolution of shell structure with changing nucleon numbers, properties of ground and excited states and electroweak transitions [20–22].

Recent microscopic shell-model studies have revealed the impact of chiral 3N forces in predicting ground- and excited-state properties in neutron- and proton-rich nuclei [1, 2, 23–27]. Despite the novel insights gained from these studies, they make approximations which are difficult to benchmark. This is because the microscopic derivation of the effective valence-space Hamiltonian relies on many-body perturbation theory (MBPT) [28], where order-by-order convergence is not clear. Even with efforts to calculate particular classes of diagrams nonperturbatively [29], results will still be sensitive to the harmonic-oscillator frequency $\hbar\omega$ (due to the core), and the choice of valence space [2, 23, 24].

To overcome these limitations, it was recently shown how the in-medium similarity renormalization group (IM-SRG) method, originally developed for *ab initio* calculations of ground states in closed-shell systems [30], can be extended to provide a nonperturbative framework to derive effective valence-space Hamiltonians and operators. The first proof-of-principle calculations in Ref. [31] focused on ^{6}Li and ^{18}O without initial 3N forces and gave promising indications that an *ab initio* description of ground- and excited-states for open-shell nuclei may be possible with this approach. In this Letter, we apply the IM-SRG starting from chiral nucleon-nucleon (NN) and 3N forces to the more challenging and physically interesting problem of the oxygen isotopes, where recent experiments have revealed the emergence of exciting new physics near and beyond stability [32–36].

In-Medium SRG. The IM-SRG consists of a continuous unitary transformation $U(s)$, parameterized by a flow parameter s, that drives the Hamiltonian to a band- or block-diagonal form [37]. This is accomplished by solving the flow equation

$$\frac{dH(s)}{ds} = [\eta(s), H(s)], \qquad (1)$$

where $\eta(s) \equiv [dU(s)/ds] \, U^\dagger(s)$ is the anti-Hermitian generator of the transformation. With a suitable choice of $\eta(s)$, the off-diagonal part of the Hamiltonian, $H^{\mathrm{od}}(s)$, is driven to zero as the flow parameter s approaches ∞. The "in-medium" label derives from the fact that we control the proliferation of induced many-body operators by normal ordering the Hamiltonian with respect to a finite-density reference state for each A-body system of interest. We truncate Eq. (1) to normal-ordered two-body operators, which we refer to as the IM-SRG(2) approximation.

The utility of the IM-SRG stems from the fact that one can tailor the definition of H^{od} to drive the Hamiltonian to a convenient form for a given problem. For instance, to construct a shell-model Hamiltonian for a nucleus comprised of A_v valence nucleons outside a closed core, we define a Hartree-Fock (HF) reference state $|\Phi\rangle$ for the core with A_c particles, and split the single-particle basis in our calculation into hole (h) as well as valence (v) and non-valence (q) particle states. Since the core is inert in a shell-model calculation, we must eliminate all matrix elements which couple $|\Phi\rangle$ to excitations, just as in the ground-state calculations discussed in [13, 14, 30]. In addition, we need to decouple states with A_v particles in the valence space, $:a_{v_1}^\dagger \ldots a_{v_{A_v}}^\dagger:|\Phi\rangle$, from states containing non-valence, i.e., q states.

Normal-ordering the Hamiltonian with respect to $|\Phi\rangle$ and working in the IM-SRG(2) truncation

$$H(s) = E_0 + \sum_{ij} f_{ij} \; :a_i^\dagger a_j: + \frac{1}{4} \sum_{ijkl} \Gamma_{ijkl} \; :a_i^\dagger a_j^\dagger a_l a_k:, \tag{2}$$

we define [31]

$$\{H^{od}\} = \{f_{ph}, f_{pp'}, f_{hh'}, \Gamma_{pp'hh'}, \Gamma_{pp'vh}, \Gamma_{pqvv'}\} + \text{H.c.} \tag{3}$$

and use the generator

$$\eta = \sum_{ij} \frac{f_{ij}^{od}}{\Delta_{ij}} \; :a_i^\dagger a_j: + \frac{1}{4} \sum_{ijkl} \frac{\Gamma_{ijkl}^{od}}{\Delta_{ijkl}} \; :a_i^\dagger a_j^\dagger a_l a_k: - \text{H.c.}, \tag{4}$$

where Δ_{ij} and Δ_{ijkl} are Epstein-Nesbet energy denominators (see Refs. [13, 30, 31]). With this choice of generator, $H^{od}(\infty) \to 0$, and the shell-model Hamiltonian is obtained by taking all valence-space matrix elements.

Implementation. For our calculations, we start from the chiral NN interaction at next-to-next-to-next-to-leading order (N³LO) by Entem and Machleidt, with cutoff $\Lambda_{NN} = 500$ MeV [4, 38], and soften it by applying a free-space SRG evolution to lower the momentum resolution scale, λ_{SRG}. Three-nucleon forces which are induced by the evolution are included consistently; we refer to this as the NN+3N-induced Hamiltonian in the following. Results for this interaction correspond to the unevolved NN interaction, up to truncated induced 4N,…,AN forces [39, 40]. The NN+3N-full Hamiltonian, in contrast, also includes an initial local chiral 3N interaction at next-to-next-to-leading order (N²LO) [41], and is consistently evolved to λ_{SRG} at the 3N level.

As discussed in Refs. [42, 43], we use the cutoff $\Lambda_{3N} = 400$ MeV in the initial 3N interaction to avoid issues with induced 4N interactions in the free-space evolution. The SRG-evolved Hamiltonians are transformed into an angular-momentum-coupled basis built from single-particle spherical harmonic-oscillator states with quantum numbers $e = 2n + l \leq e_{max}$. An additional cut $e_1 + e_2 + e_3 \leq E_{3max} < 3e_{max}$ is introduced to

TABLE I. IM-SRG sd-shell SPEs (in MeV) for $\lambda_{SRG} = 1.88\,\text{fm}^{-1}$ and $\hbar\omega = 24\,\text{MeV}$, compared with MBPT [23] (NN+3N, see text) and phenomenological USDb values [45].

Orbit	NN	NN+3N-ind.	NN+3N-full	MBPT	USDb
$d_{5/2}$	−7.90	−3.77	−4.62	−3.78	−3.93
$s_{1/2}$	−6.87	−2.46	−2.96	−2.42	−3.21
$d_{3/2}$	1.41	2.33	3.17	1.45	2.11

manage the storage requirements of the 3N matrix elements. Throughout this work, we use $E_{3max} = 14$, which for resolution scales $\lambda_{SRG} = 1.88 - 2.24$ fm⁻¹ gives converged ground states with uncertainty of less than 1% [10, 12–14, 18].

The first step in our calculations is solving the HF equations for a closed-shell core, here ¹⁶O. In the Hamiltonian, we use the intrinsic kinetic energy,

$$T_{int} = T - T_{cm} = \left(1 - \frac{1}{A}\right) \sum_i \frac{\boldsymbol{p}_i^2}{2m} - \frac{1}{Am} \sum_{i<j} \boldsymbol{p}_i \cdot \boldsymbol{p}_j, \tag{5}$$

with A being the particle number of the *target nucleus* rather than the core, in order to account for the change of the single-particle wavefunctions as $A_c \to A$ [44]. The Hamiltonian is then normal ordered with respect to the core's HF reference state, and the resulting in-medium zero-, one-, and two-body operators serve as the initial values for the IM-SRG flow equations. The residual three-body term is neglected, giving rise to the normal-ordered two-body (NO2B) approximation [7, 10, 12].

The one- and two-body parts of the fully decoupled ($s \to \infty$) valence-space Hamiltonian are taken as the single-particle energies (SPEs) and two-body matrix elements, respectively, to be diagonalized exactly in a standard shell-model calculation. We restrict ourselves to a valence space comprised of the $d_{5/2}$, $d_{3/2}$, and $s_{1/2}$ orbitals (the sd shell) above an inert ¹⁶O core. We specifically show IM-SRG(2) results for Hamiltonians with $\lambda_{SRG} = 1.88\,\text{fm}^{-1}$, because the spectra are insensitive to variations of the resolution scale. Energy levels for $\lambda_{SRG} = 2.24$ fm⁻¹ typically differ by $30 - 50\,\text{keV}$, with only two instances of deviations of 100 keV. Of greater interest is the $\hbar\omega$-dependence of the spectra, because $\hbar\omega$ is adjusted to the core in phenomenological shell-model calculations. We illustrate the effect of varying $\hbar\omega$ from 20 MeV to 24 MeV by shaded bands in the following plots. Since this variation probes the convergence of the calculation, and is mainly governed by λ_{SRG} rather than the specific input Hamiltonian, we only show these bands for the NN+3N-full Hamiltonian.

Results. The IM-SRG SPEs for the NN, NN+3N-induced, and NN+3N-full Hamiltonians are given in Table I and compared to those calculated in MBPT, using a softened N³LO NN interaction and a re-fit N²LO 3N interaction (see Refs. [1, 2, 39] for details), and values from
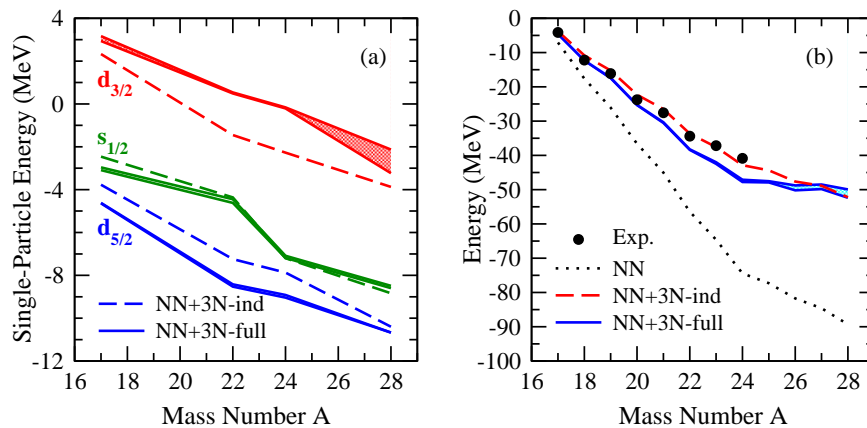
FIG. 1. (Color online) Single-particle energy evolution (a) and ground-state energies (b) for A-dependent Hamiltonian with $\lambda_{\mathrm{SRG}} = 1.88\,\mathrm{fm}^{-1}$. The range of NN+3N-full results for $\hbar\omega = 20, 24\,\mathrm{MeV}$ is given by the shaded bands.

the phenomenological USDb Hamiltonian [45]. Similar to the MBPT calculations, in the NN case, the IM-SRG SPEs are significantly overbound with $\lambda_{\mathrm{SRG}} = 1.88\,\mathrm{fm}^{-1}$ (e.g., the $d_{5/2}$ orbital is 4 MeV lower than in USDb). In the NN+3N-full case, the resulting SPEs are now comparable to MBPT and phenomenology. The $d_{5/2} - d_{3/2}$ gap is approximately 2 MeV larger in IM-SRG, pointing to a stronger spin-orbit component, while the $d_{5/2} - s_{1/2}$ gap is similar to that in MBPT, being almost 1 MeV larger than in USDb. The variation of the IM-SRG SPEs with respect to $\lambda_{\mathrm{SRG}} = 1.88 - 2.24\,\mathrm{fm}^{-1}$ and $\hbar\omega = 20 - 24\,\mathrm{MeV}$ results in small changes in $d_{5/2}$ of less than 100 keV and in $d_{3/2}$ and $s_{1/2}$ of less than 300 keV.

Insights into the structure towards the exotic region can be gained from the evolution of the SPEs as a function of neutron number, shown in Fig. 1(a). The importance of 3N forces in determining the oxygen dripline was highlighted in microscopic valence-space calculations [1, 23] and *ab initio* ground-state calculations [8, 14, 15]. Here we find a similar mechanism at work: in the NN+3N-induced case, the $d_{3/2}$ orbit remains bound throughout the isotopic chain, in particular past ^{24}O. In contrast, the repulsive effects of 3N forces shift the $d_{3/2}$ orbit to a relatively high starting point of 3.17 MeV in ^{17}O, while moderating its decrease to neutron-rich isotopes, where it becomes bound by only 160 keV in ^{24}O.

We now diagonalize the A-dependent IM-SRG valence-space Hamiltonian to obtain the ground-state energies, relative to ^{16}O, of the oxygen isotopes $^{18-28}$O. The results, shown in Fig. 1(b), highlight the predictive power of IM-SRG as well as the decisive role of 3N forces. For an SRG-evolved NN interaction with $\lambda_{\mathrm{SRG}} = 1.88\,\mathrm{fm}^{-1}$ alone, the oxygen isotopes are progressively overbound throughout the chain due to the neglect of both initial and induced 3N forces, leading to unrealistic predictions in the neutron-rich region. Including induced 3N forces lessens the overbinding, but fails to give the correct location of the dripline. With initial 3N forces included, the agreement with experimental data is remarkably good,

though moderate overbinding is observed past ^{22}O. Furthermore, the flat trend of the ground-state energies beyond ^{24}O is similar to the experimental data in ^{25,26}O [33–35] and agrees well with other many-body calculations based on chiral NN+3N forces [1, 8, 15, 23]. We note, however, that $^{25-28}$O are weakly bound w.r.t. ^{24}O; the ground state of ^{26}O lies 90 keV below that of ^{24}O.

This result is in contrast with the multi-reference IM-SRG (MR-IM-SRG) results of Ref. [14], which give a robust prediction of the dripline in ^{24}O with the same Hamiltonian. Overall, the ground-state energies calculated from the IM-SRG valence-space Hamiltonians are slightly below those from MR-IM-SRG, which are in very good agreement with experimental data and other *ab initio* methods [14]. Of course, the MR-IM-SRG evolution is carried out in the target nucleus rather than in the core with shifted A. Its open-shell reference state accounts for wavefunction relaxation effects, as well as the presence of nucleons in the valence-shell during the evolution. Therefore differences, especially for neutron-rich systems far from the ^{16}O core, are to be expected, although they only amount to 2 % at most. In the future, we will revisit this issue by using ^{22}O and ^{24}O cores with a suitably adapted IM-SRG generator, and compare our present results with MR-IM-SRG results for excited states.

In Fig. 1(b), we highlight the insensitivity of the ground-state energies to a variation of the harmonic-oscillator parameter from $\hbar\omega = 20$ MeV to 24 MeV by showing a band for the NN+3N-full Hamiltonian. Differences due to this range of $\hbar\omega$ values only become non-negligible for very neutron-rich systems, growing from approximately 650 keV in ^{24}O to 1.9 MeV in ^{28}O. The relative independence of calculated observables with respect to $\hbar\omega$ is a striking feature of the nonperturbative IM-SRG valence-space approach, implying a remarkable level of convergence already at the IM-SRG(2) level.

We now turn to excitation spectra in the oxygen isotopes. Since it is well known that NN forces already give a reasonable description of low-lying spectra near ^{16}O [28],

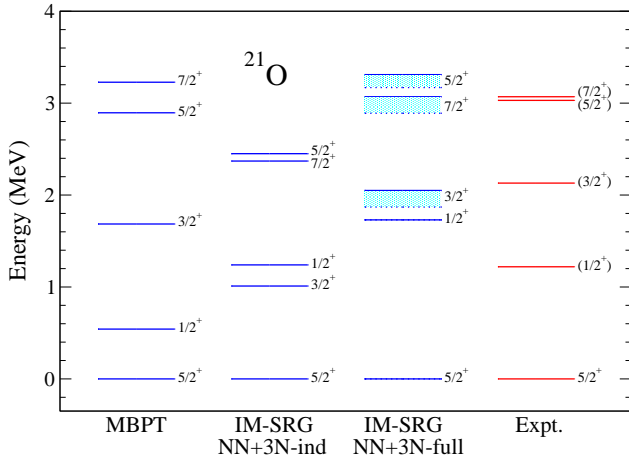FIG. 2. (Color online) Excited state spectrum of ^{21}O for IM-SRG Hamiltonians based on NN+3N-induced and NN+3N-full inputs, with $\hbar\omega = 20\,\mathrm{MeV}$ (dotted) and $\hbar\omega = 24\,\mathrm{MeV}$ (solid), compared with MBPT (NN+3N) and experiment [46].

by considering $^{21-26}$O we focus on the region of the new $N = 14, 16$ magic numbers and beyond stability. It was shown in Ref. [23] that microscopic valence-space Hamiltonians calculated in the standard sd-shell did not adequately reproduce the experimental data, even when 3N forces were considered. Instead, single-particle orbitals from above the sd-shell, namely $f_{7/2}$ and $p_{3/2}$, when included, improved spectroscopy, indicating that a perturbative treatment of these orbitals may not be sufficient. Given the nonperturbative character of the IM-SRG, we expect similar improvements already in the sd shell.

We first consider the spectrum of ^{21}O in Fig. 2, which can be considered as a $d_{5/2}$ particle coupled to ^{20}O. While no calculation fully reproduces experiment, MBPT and IM-SRG predict the correct ordering of the first two excited states if an initial 3N force is present, but with the $1/2^+$ too low in MBPT and too high in IM-SRG. Recall
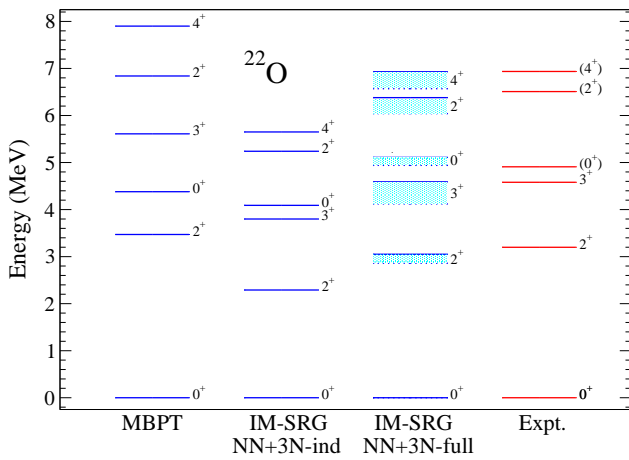

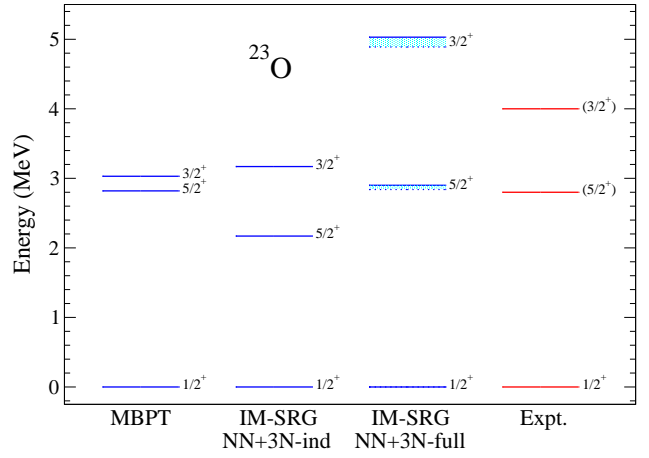FIG. 3. (Color online) Excited state spectrum for ^{22}O as in Fig. 2, with experimental values taken from [46, 47].

FIG. 4. (Color online) Excited state spectrum of ^{23}O as in Fig. 2, with experimental values taken from [48, 49].

that the MBPT is based on a softened N^{3}LO interaction with a re-fit 3N interaction [1, 2], so the difference is due to the different input Hamiltonians as well as the non-perturbative IM-SRG approach. The two effects will be investigated and disentangled in future work. We also note that the tentative $7/2^+$ and $5/2^+$ spin assignments are reproduced in both calculations, but the ordering is reversed in IM-SRG compared to MBPT.

We show the calculated IM-SRG ^{22}O spectra compared with MBPT [23] and experiment [46, 47] in Fig. 3. Without the initial 3N force, the spectrum is too compressed with respect to experiment, where in particular the 2_1^+ state is 1.0 MeV too low, not reproducing the doubly magic nature of ^{22}O. It is interesting to note, however, that the correct ordering of the 3_1^+ and 0_2^+ states is reproduced, a feature not seen in either MBPT or the phenomenological USDb Hamiltonian. When the initial 3N force is included in the IM-SRG, we see significant improvement, where the final spectrum is very close to experiment, in contrast to that of the extended-space MBPT calculations, which reproduce the high 2_1^+ state but have too uniform spacing and an incorrect $3_1^+ - 0_2^+$ ordering.

There are no bound excited states observed in ^{23}O, and only two higher-lying states, which have been tentatively identified as $5/2^+$ and $3/2^+$, indicating the sizes of the $d_{5/2} - s_{1/2}$ and $d_{3/2} - s_{1/2}$ gaps respectively [48, 49]. We show the calculated and experimental ^{23}O spectrum in Fig. 4, where again without the initial 3N force, IM-SRG does not reproduce this spectrum well, with the $5/2^+$ being nearly 1 MeV too low, but the $5/2^+ - 3/2^+$ gap close to experiment. Similar to the MBPT calculation, with the initial 3N force, the $5/2^+$ energy is almost exactly that of experiment, only now the $3/2^+$ is 1 MeV too high rather than 1 MeV too low. Due to its position 2 MeV above threshold, however, it is expected that continuum effects, when included, will lower the energy of this state, bringing it closer to the experimentally observed value.
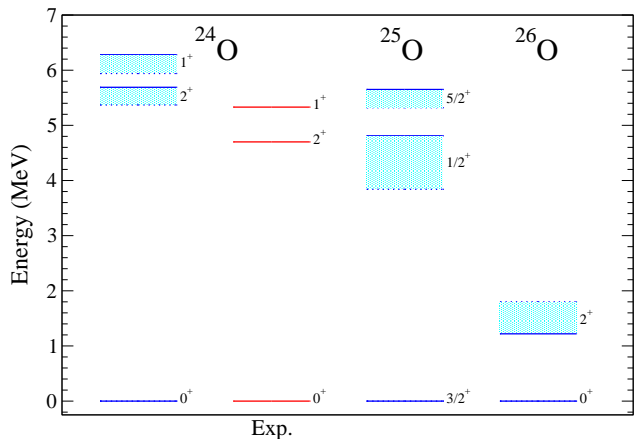
FIG. 5. (Color online) Excited state spectra of $^{24-26}$O for the NN+3N-full Hamiltonian, with $\hbar\omega = 20\,\mathrm{MeV}$ (dotted) $\hbar\omega = 24\,\mathrm{MeV}$ (solid), compared to experiment for ^{24}O [32].

As expected from the high $3/2^+$ state in ^{23}O, we also predict ^{24}O to be doubly magic, but with a 2_1^+ energy $1.2\,\mathrm{MeV}$ higher than experiment as seen in Fig. 5. Nonetheless, the $2^+ - 1^+$ spacing is very close to experiment and with continuum effects included, these states will be lowered. Finally, we present predictions for excited-state energies in the unbound ^{25,26}O isotopes. We again find large $1/2^+$ and $5/2^+$ excitation energies in ^{25}O, which are expected to decrease with continuum coupling. In ^{26}O, we predict one low-lying state below $6\,\mathrm{MeV}$: a 2^+ just below $2\,\mathrm{MeV}$. A tentative identification of an excited state near $4\,\mathrm{MeV}$ was reported in [35], but no such natural-parity state was found in our calculations.

Conclusions. We have presented the first *ab initio* construction of a nonperturbative *sd*-shell Hamiltonian based on chiral NN and 3N forces. The SPEs and two-body matrix elements are very well converged with respect to basis size and exhibit a weak $\hbar\omega$ dependence. Furthermore, a very good description of ground and excited states is found throughout the chain of oxygen isotopes in a valence space consisting of only the *sd*-shell orbits. This provides the exciting possibility to extend these calculations to nearby F, Ne, and Mg isotopic chains and through extending the valence space, will give access to the island-of-inversion region and potentially the full *sd*-shell neutron dripline.

* E-mail: bogner@nscl.msu.edu
† E-mail: hergert.3@osu.edu
‡ E-mail: jason.holt@physik.tu-darmstadt.de
§ E-mail: schwenk@physik.tu-darmstadt.de

[1] T. Otsuka, T. Suzuki, J. D. Holt, A. Schwenk, and Y. Akaishi, Phys. Rev. Lett. **105**, 032501 (2010)
[2] J. D. Holt, T. Otsuka, A. Schwenk, and T. Suzuki, J. Phys. G **39**, 085111 (2012)
[3] E. Epelbaum, H.-W. Hammer, and U.-G. Meißner, Rev. Mod. Phys. **81**, 1773 (2009)
[4] R. Machleidt and D. Entem, Phys. Rept. **503**, 1 (2011)
[5] H.-W. Hammer, A. Nogga, and A. Schwenk, Rev. Mod. Phys. **85**, 197 (2013)
[6] G. Hagen, T. Papenbrock, D. J. Dean, and M. Hjorth-Jensen, Phys. Rev. C **82**, 034330 (2010)
[7] G. Hagen, T. Papenbrock, D. J. Dean, A. Schwenk, A. Nogga, M. Włoch, and P. Piecuch, Phys. Rev. C **76**, 034302 (2007)
[8] G. Hagen, M. Hjorth-Jensen, G. Jansen, R. Machleidt, and T. Papenbrock, Phys. Rev. Lett. **108**, 242501 (2012)
[9] G. Hagen, M. Hjorth-Jensen, G. Jansen, R. Machleidt, and T. Papenbrock, Phys. Rev. Lett. **109**, 032502 (2012)
[10] R. Roth, S. Binder, K. Vobig, A. Calci, J. Langhammer, and P. Navrátil, Phys. Rev. Lett. **109**, 052501 (2012)
[11] V. Somá, C. Barbieri, and T. Duguet, Phys. Rev. C **87**, 011303 (2013)
[12] S. Binder, J. Langhammer, A. Calci, P. Navrátil, and R. Roth, Phys. Rev. C **87**, 021303 (2013)
[13] H. Hergert, S. K. Bogner, S. Binder, A. Calci, J. Langhammer, R. Roth, and A. Schwenk, Phys. Rev. C **87**, 034307 (2013)
[14] H. Hergert, S. Binder, A. Calci, J. Langhammer, and R. Roth, Phys. Rev. Lett. **110**, 242501 (2013)
[15] A. Cipollone, C. Barbieri, and P. Navrátil, Phys. Rev. Lett. **111**, 062501 (2013)
[16] G. R. Jansen, Phys. Rev. C **88**, 024305 (2013)
[17] V. Somá, A. Cipollone, C. Barbieri, P. Navrátil, and T. Duguet(2013), arXiv:1312.2068 [nucl-th]
[18] S. Binder, J. Langhammer, A. Calci, and R. Roth(2013), arXiv:1312.5685 [nucl-th]
[19] G. Hagen, T. Papenbrock, M. Hjorth-Jensen, and D. Dean(2013), arXiv:1312.7872 [nucl-th]
[20] B. A. Brown, Prog. Part. Nucl. Phys. **47**, 517 (2001)
[21] E. Caurier, G. Martinez-Pinedo, F. Nowacki, A. Poves, and A. Zuker, Rev. Mod. Phys. **77**, 427 (2005)
[22] T. Otsuka, Physica Scripta **2013**, 014007 (2013)
[23] J. D. Holt, J. Menéndez, and A. Schwenk, Eur. Phys. J. **A49**, 39 (2013)
[24] J. D. Holt, J. Menéndez, and A. Schwenk, Phys. Rev. Lett. **110**, 022502 (2013)
[25] J. D. Holt, J. Menéndez, and A. Schwenk, J. Phys. G **40**, 075105 (2013)
[26] A. Gallant, J. Bale, T. Brunner, U. Chowdhury, S. Ettenauer, *et al.*, Phys. Rev. Lett. **109**, 032506 (2012)
[27] F. Wienholtz, D. Beck, K. Blaum, C. Borgmann, M. Breitenfeldt, *et al.*, Nature **498**, 346 (2013)

[28] M. Hjorth-Jensen, T. Kuo, and E. Osnes, Phys. Rept. **261**, 125 (1995)

[29] J. D. Holt, J. W. Holt, T. T. S. Kuo, G. E. Brown, and S. K. Bogner, Phys. Rev. C **72**, 041304 (2005)

[30] K. Tsukiyama, S. K. Bogner, and A. Schwenk, Phys. Rev. Lett. **106**, 222502 (2011)

[31] K. Tsukiyama, S. K. Bogner, and A. Schwenk, Phys. Rev. C **85**, 061304(R) (2012)

[32] C. Hoffman, T. Baumann, D. Bazin, J. Brown, G. Christian, *et al.*, Phys. Rev. Lett. **100**, 152502 (2008)

[33] R. Kanungo, C. Nociforo, A. Prochazka, T. Aumann, D. Boutin, *et al.*, Phys. Rev. Lett. **102**, 152501 (2009)

[34] E. Lunderberg, P. DeYoung, Z. Kohley, H. Attanayake, T. Baumann, *et al.*, Phys. Rev. Lett. **108**, 142503 (2012)

[35] C. Caesar *et al.* (R3B collaboration), Phys. Rev. C **88**, 034313 (2013)

[36] Z. Kohley, G. Christian, T. Baumann, P. A. DeYoung, J. E. Finck, *et al.*, Phys. Rev. Lett. **110**, 152501 (2013)

[37] S. K. Bogner, R. J. Furnstahl, and R. J. Perry, Phys. Rev. C **75**, 061001(R) (2007)

[38] D. R. Entem and R. Machleidt, Phys. Rev. C **68**, 041001 (2003)

[39] S. K. Bogner, R. J. Furnstahl, and A. Schwenk, Prog. Part. Nucl. Phys. **65**, 94 (2010)

[40] E. D. Jurgenson, P. Navrátil, and R. J. Furnstahl, Phys. Rev. Lett. **103**, 082501 (2009)

[41] P. Navrátil, Few-Body Systems **41**, 117 (2007)

[42] R. Roth, J. Langhammer, A. Calci, S. Binder, and P. Navrátil, Phys. Rev. Lett. **107**, 072501 (2011)

[43] R. Roth, A. Calci, J. Langhammer, and S. Binder(2013), arXiv:1311.3563 [nucl-th]

[44] H. Hergert and R. Roth, Phys. Lett. B **682**, 27 (2009), arXiv:0908.1334 [nucl-th]

[45] B. A. Brown and W. Richter, Phys. Rev. C **74**, 034315 (2006)

[46] M. Stanoiu, F. Azaiez, Z. Dombradi, O. Sorlin, B. A. Brown, *et al.*, Phys. Rev. C **69**, 034312 (2004)

[47] B. Fernandez-Dominguez, J. Thomas, W. Catford, F. Delaunay, S. Brown, *et al.*, Phys. Rev. C **84**, 011301 (2011)

[48] Z. Elekes, Z. Dombradi, N. Aoi, S. Bishop, Z. Fulop, *et al.*, Phys. Rev. Lett. **98**, 102502 (2007)

[49] A. Schiller, N. Frank, T. Baumann, D. Bazin, B. A. Brown, *et al.*, Phys. Rev. Lett. **99**, 112501 (2007)